Effects of pore fluid chemistry on localised and ductile deformation of porous rocks.

Francesco Lazari[1*], Gabriel Meyer[1,2], Anne Pluymakers[3], Lukas P. Baumgartner[4], Marie Violay[1].

[1]: LEMR, EPFL, Lausanne, Switzerland
[2]: Njord Centre, University of Oslo, Norway
[3]: CiTG, TU Delft, Netherlands
[4]:Institute of Earth Sciences, University of Lausanne, Switzerland
* corresponding author: francesco.lazari@epfl.ch

EGU General Assembly

Swiss National Science Foundation

This presentation participates in OSPP

Outstanding Student & PhD candidate Presentation contest

Introduction

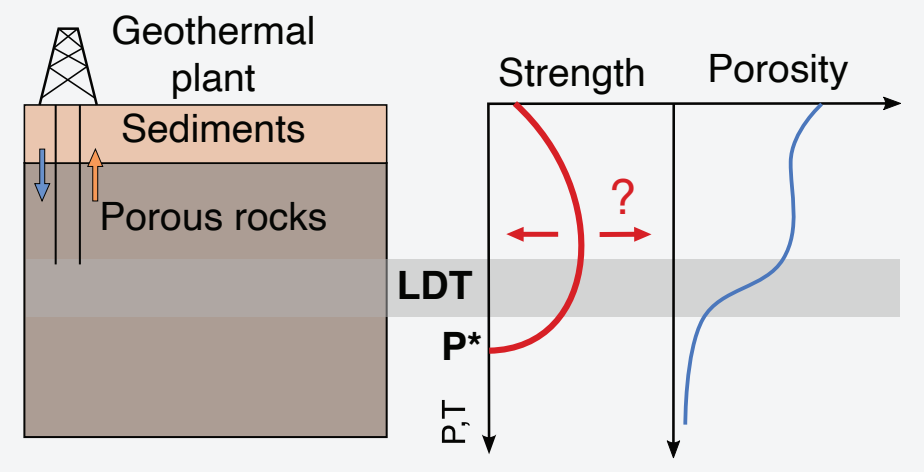

Figure 1: schematic representation of a geothermal reservoir, and the strength and porosity variations with pressure and temperature.

Geological applications such as geothermal energy and CO_2 storage operations mainly target porous rocks, where pore fluid chemistry can dramatically alter rock mechanical behavior. While siliciclastic rocks show chemical weakening primarily during ductile deformation[19], carbonates present unique challenges due to their high reactivity and rapid dissolution-precipitation kinetics.

Below critical depths (from ~2-3 km), porous reservoir rocks transition from localized failure (maintaining permeability) to ductile compaction (drastically reducing permeability). The change in deformation mode is named Localized to Ductile Transition (LDT)[20]. This transition depth controls reservoir exploitability, yet the role of fluid chemistry remains poorly constrained.
Recent works[4] reveal that carbonates are weakened by water presence , while specific ions can have have opposing effects on limestone strength[14].

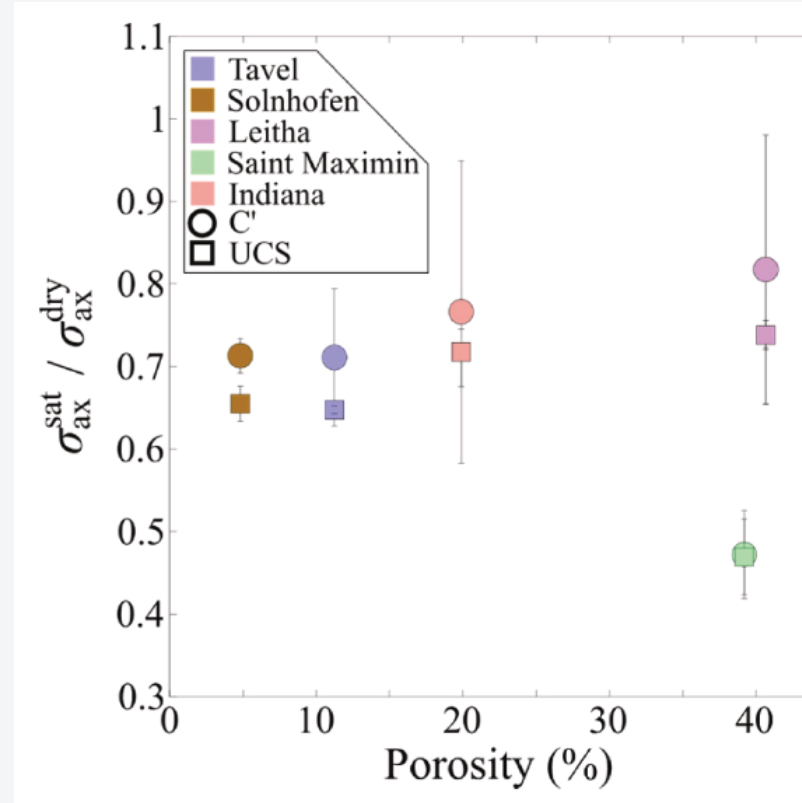

Figure 2: yield and uniaxial compressive strength weakening of different carbonates saturated with deionized water[4].

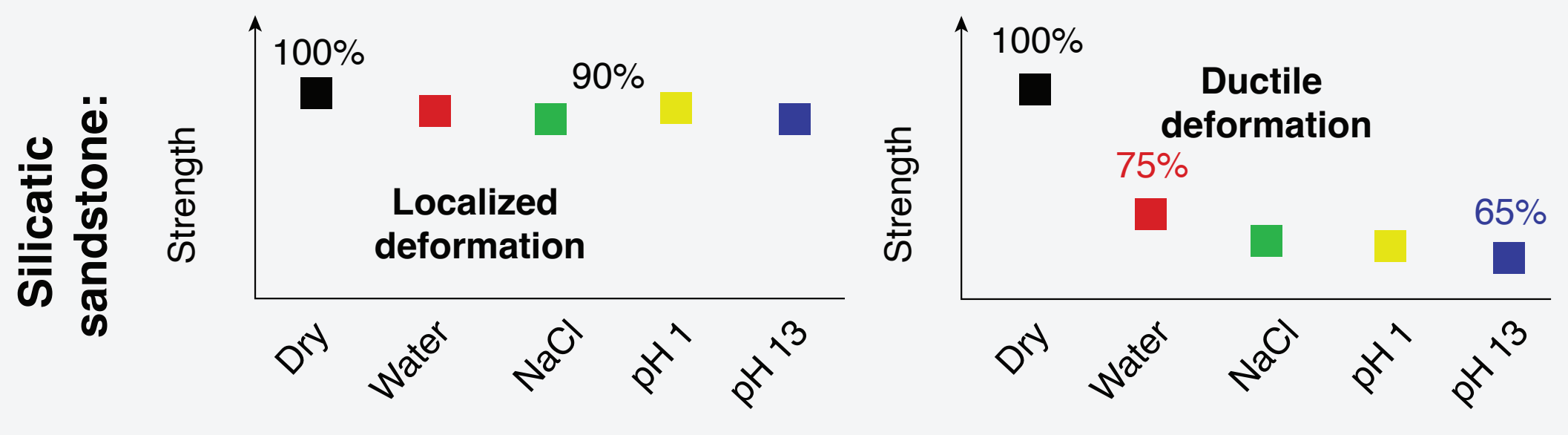

Figure 3: Strength versus fluid chemistry during localized and ductile deformation for a silicatic sandstone. Strength is affected by fluid presence and chemistry during ductile deformation. From Lazari et al. (2025).

What do we know so far about the deformation of porous carbonates? And what is the effect of different ionic species on localised and ductile deformation of porous carbonates?

Methods

We performed triaxial experiments on Tavel limestone (84% calcite, 7.5% quartz, 6% phyllosilicates) with 11 to 15% porosity, chosen for its homogeneity and fine grain size.

- $P_{c\ eff}$ of 20 MPa (localized deformation) and 100 MPa (ductile deformation) with a constant strain rate $\varepsilon'=10^{-6}$ s^{-1};
- Constant P_P 10 MPa and ΔP_P of 1 MPa to ensure fluid flow and allow for permeability calculation;
- Deformation up to ε=10%;
- Electrical conductivity measured between 0.1 Hz and 1 MHz every 15 minutes;
- Ultrasonic seismic velocity measured every 15 minutes;
- Fluid sampling at the beginning and end of each experiment.

Samples were deformed either dry or saturated with several water solutions spanning widely in pH and ionic composition:

- **0.01 M HCl** solution (pH 2);
- **deionized water with 4 MPa of CO_2** (pH 5);
- **deionized water** (pH 6);
- **CaCO3 saturated** solution (pH 7);
- **0.1 M $MgCl_2$** solution (pH 7);
- **6 M NaCl** solution (pH 7);
- **0.1 M NaOH** solution (pH 13).

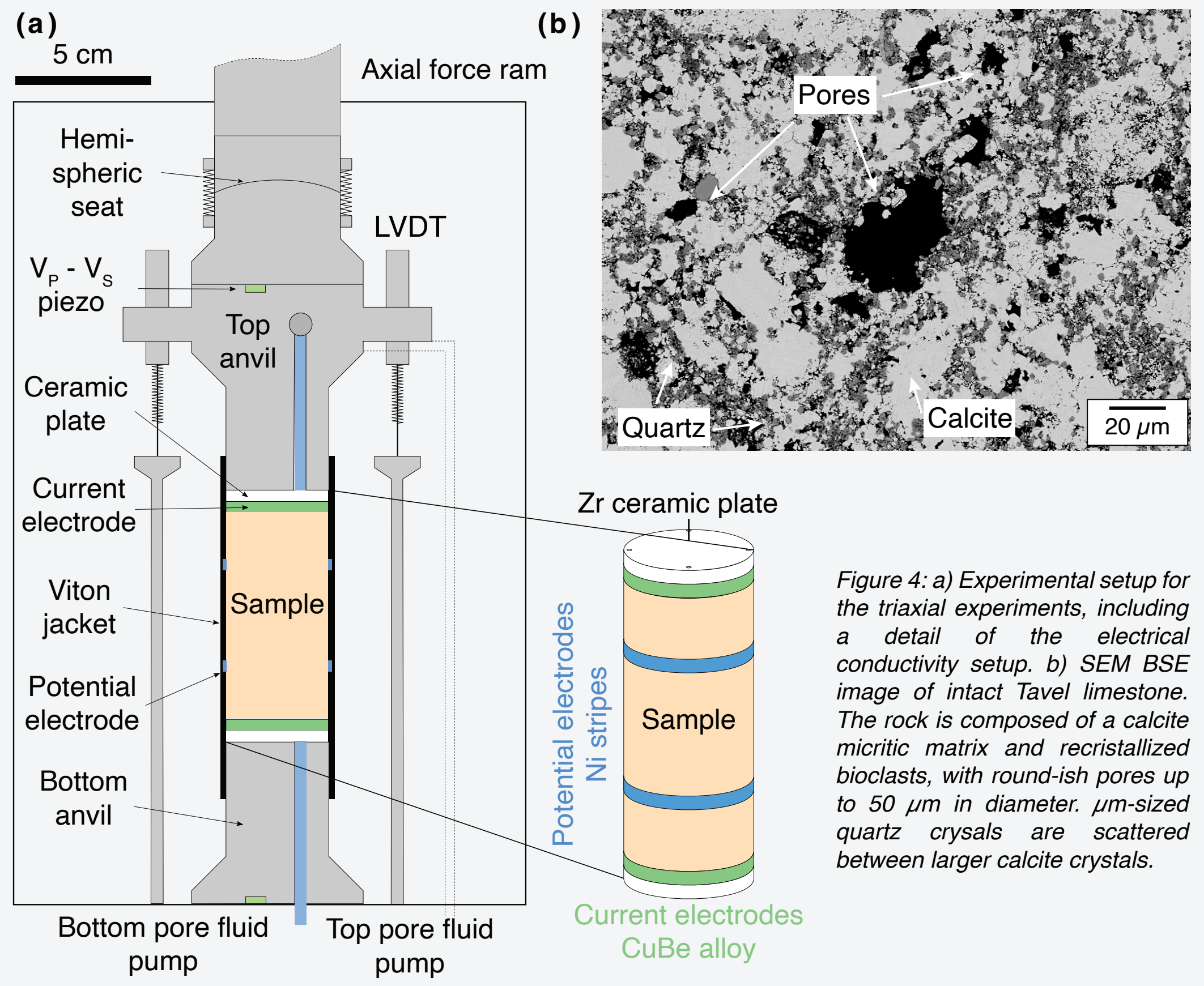

Figure 4: a) Experimental setup for the triaxial experiments, including a detail of the electrical conductivity setup. b) SEM BSE image of intact Tavel limestone. The rock is composed of a calcite micritic matrix and recristallized bioclasts, with round-ish pores up to 50 μm in diameter. μm-sized quartz crysals are scattered between larger calcite crystals.

Carbonate deformation in the literature

Triaxial experiments

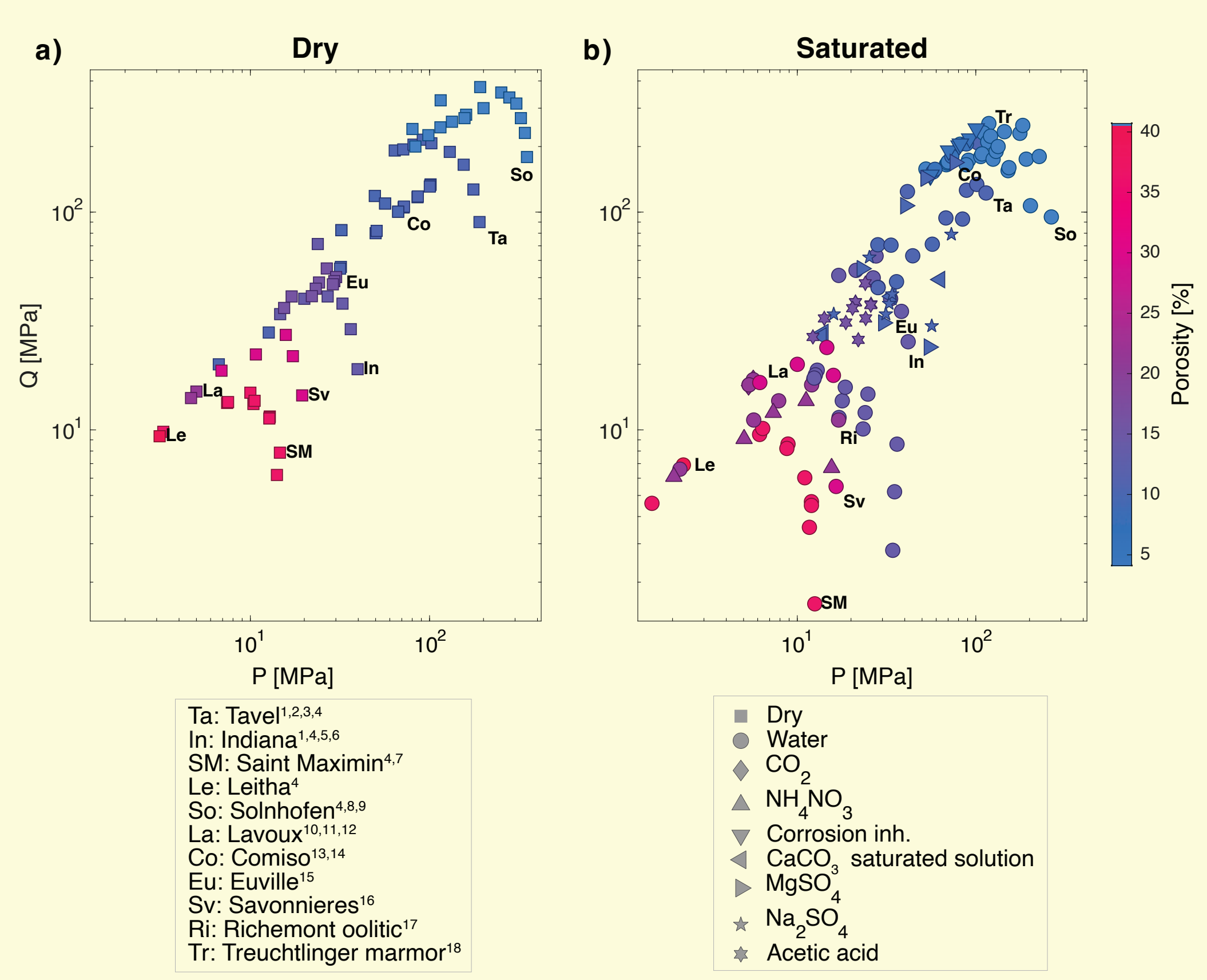

Figure 5: a) Yield P-Q diagram for constant strain rate triaxial and uniaxial experiments on various limestones from the literature, performed dry or with chemically inert fluids. b) experiments performed with acqueous solutions spanning various compositions.

Experiments on dry carbonatic rocks in the literature highlight how the failure envelope is mainly controlled by the porosity of the rock. Adding a fluid retains a first-order control of porosity but increases the scatter in the yield envelope.

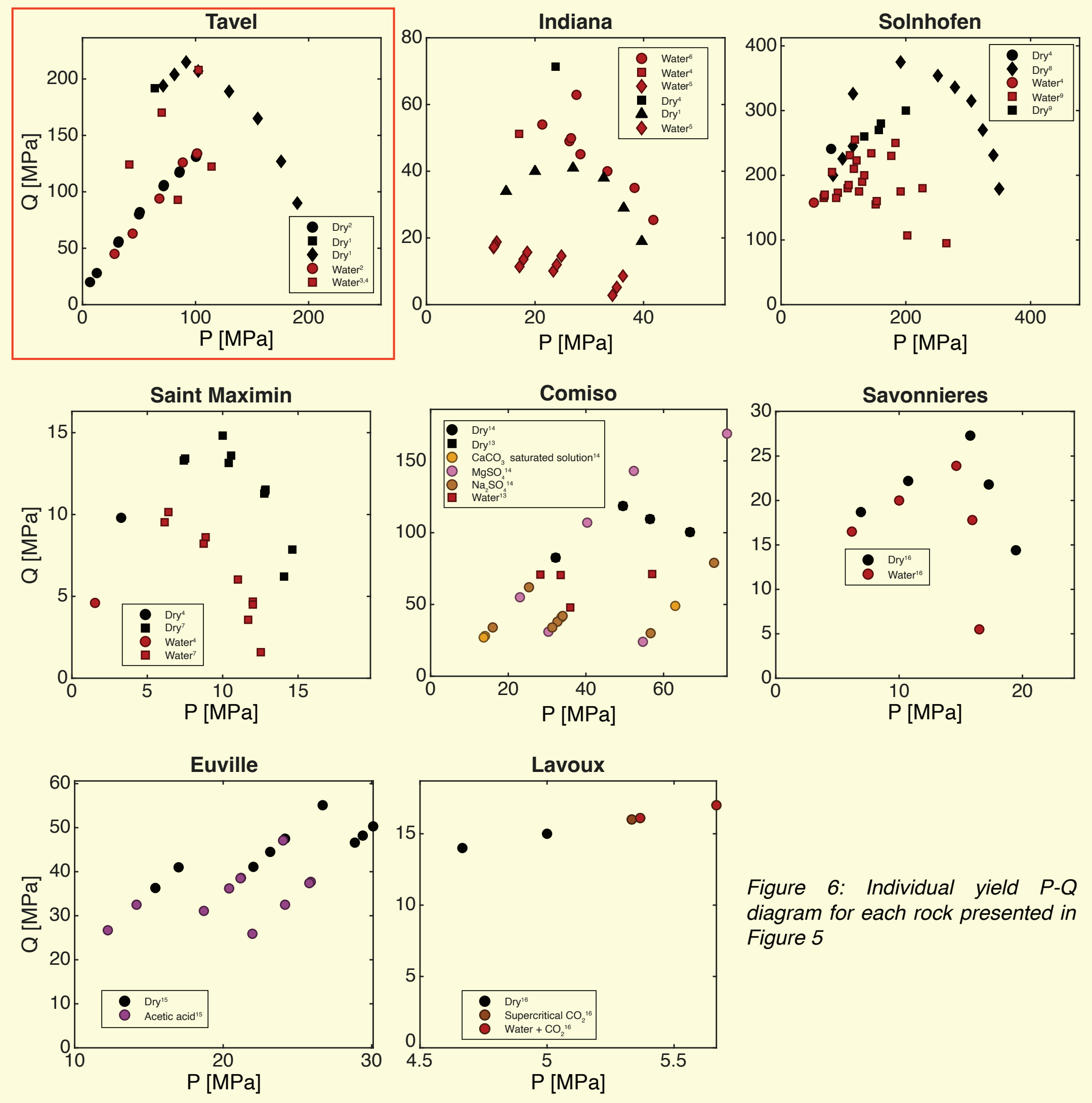

Figure 6: Individual yield P-Q diagram for each rock presented in Figure 5

Water generally weakens the strength of carbonatic rocks, but the effects are extremely rock-dependant, and cannot be generalized from the available literature data.

Micromechanical processes

Mechanism	Deionized water	NaCl low M	NaCl high M	$MgSO_4$ $MgCl_2$	$CaCl_2$ low M	Na_2SO_4 low M	Na_2SO_4 high M
Cracking [4, 23, 24]	↓	↓	↑	—	?	↑	↓
Pressure solution [25, 26, 27]	↓	↑	↓	↑	↓	?	?
Dislocation creep [29]	—	—	—	—	—	—	—
Twinning [29]	—	—	—	—	—	—	—

Localised deformation

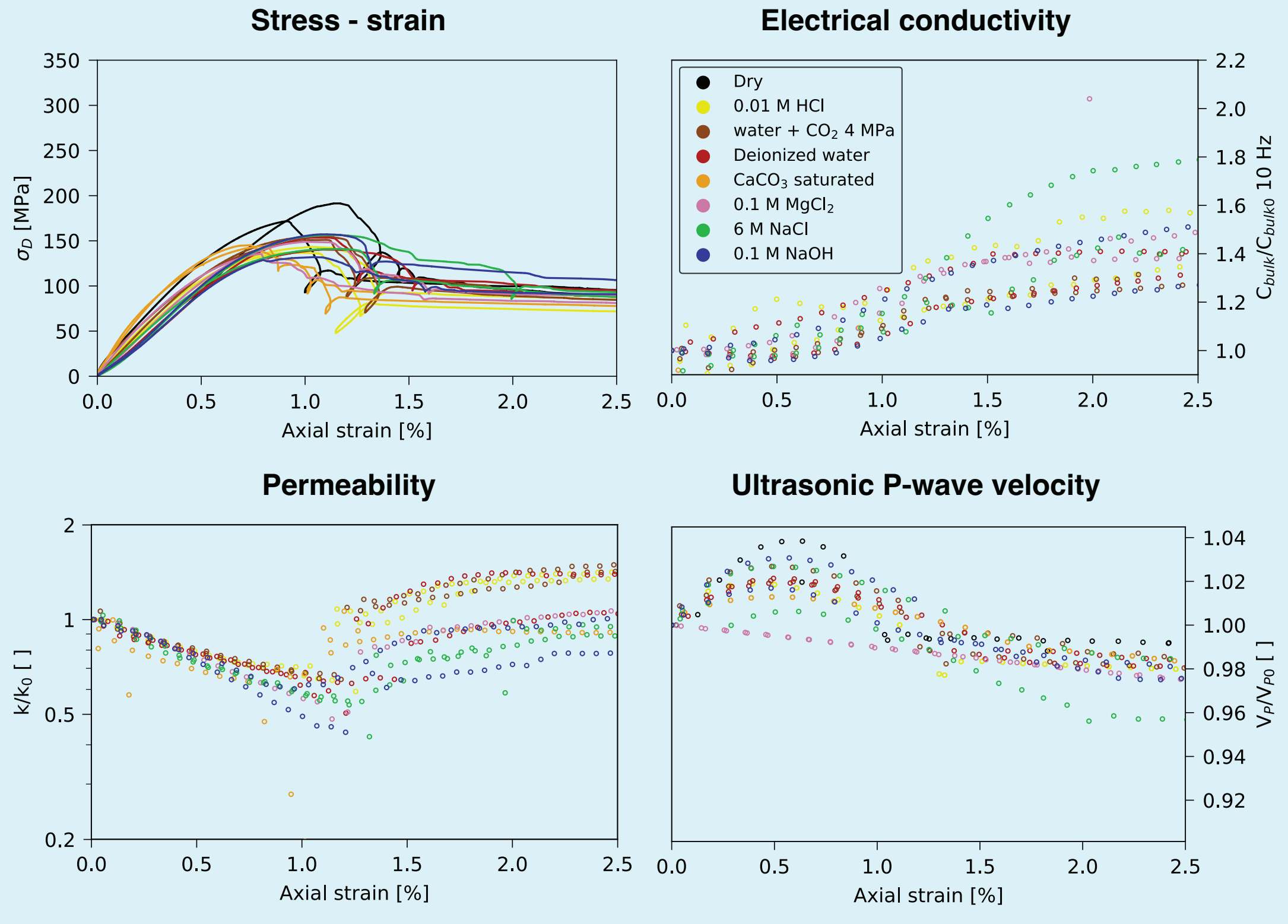

Figure 7: mechanical and physical measurements of experiments performed at $P_{c\ eff}$ = 20 MPa

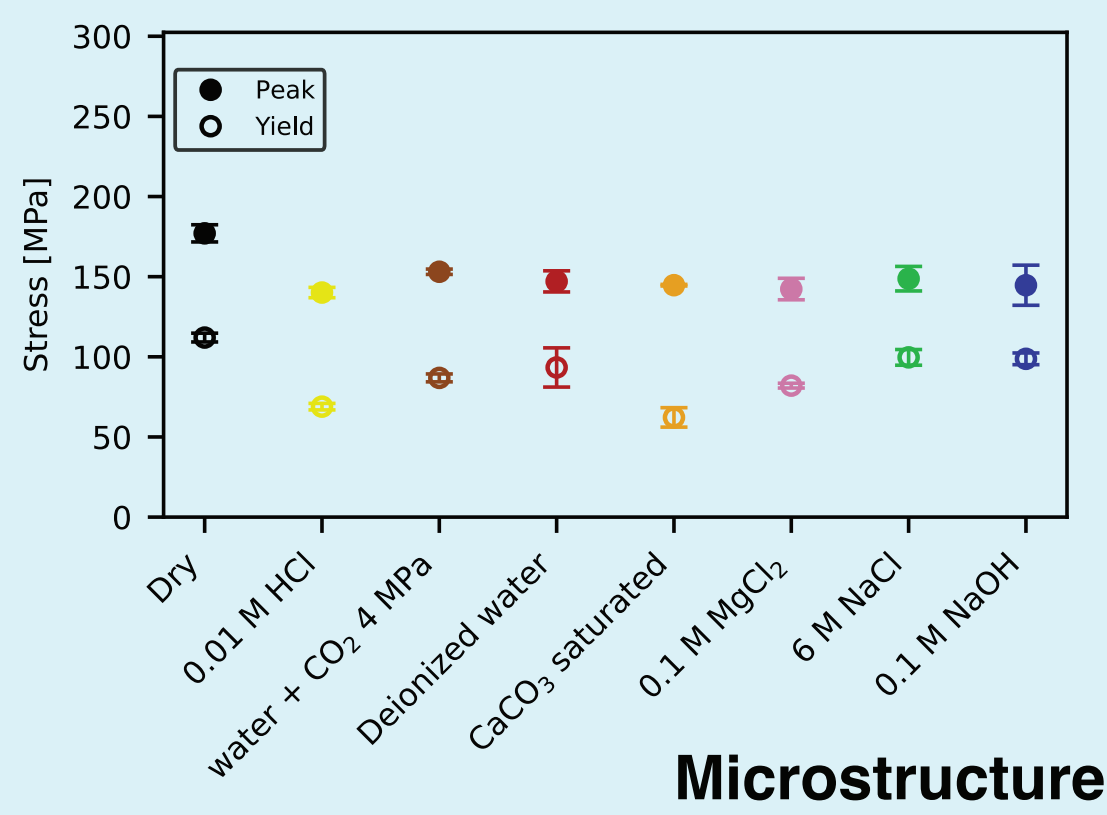

Samples saturated with a fluid have average peak stress weakening of 20% compared to dry. Yield stress of **0.01 M HCl** and **$CaCO_3$**-saturated samples is the lowest of the set, 40 to 50% weakening compared to dry.
While permeability sharply changes only upon failure, electrical conductivity and V_P can highlight the yield point of the rock, serving as a precursor to failure.

Microstructures

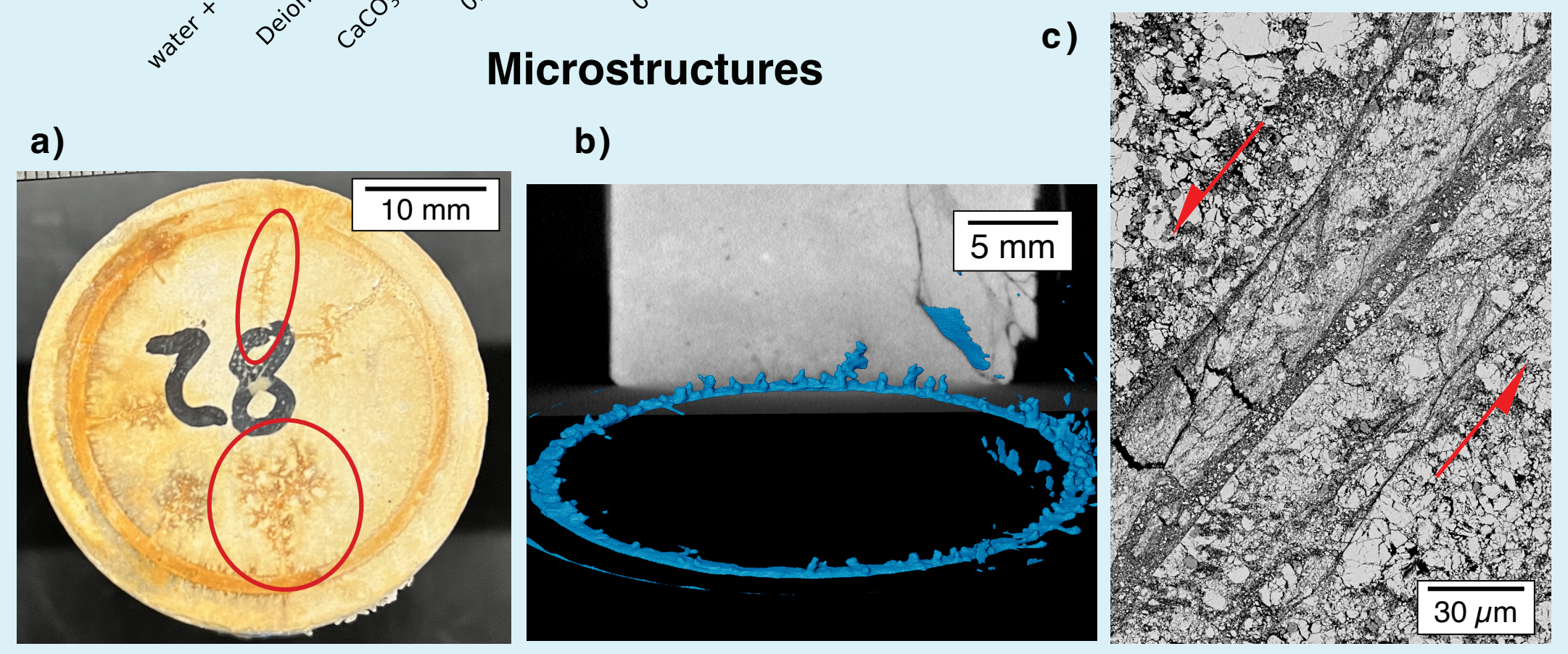

*Figure 8: a) dendritic dissolution pattern at the inlet of a sample deformed with **HCl**. b) CT scan segmentation highlighting wormholes at the inlet of a sample deformed with **water and CO_2**. c) SEM BSE of a sample deformed with **deionized water**, showing a shear band filled with gouge.*

Samples deformed with **HCl** present superficial dendritic dissolution patter at the downstream side of the sample, indicating fast dissolution happening at the fluid inlet. Samples deformed with **water and CO_2** show wormholes a few mm deep, concentrated closer to the shear fracture. Samples deformed with other solutions don't show macroscopically visible features besides the shear fracture. At the microscope, all samples present one or multiple shear fractures filled with gouge, as well as twinned crystals next to the shear zone.

Porosity effect

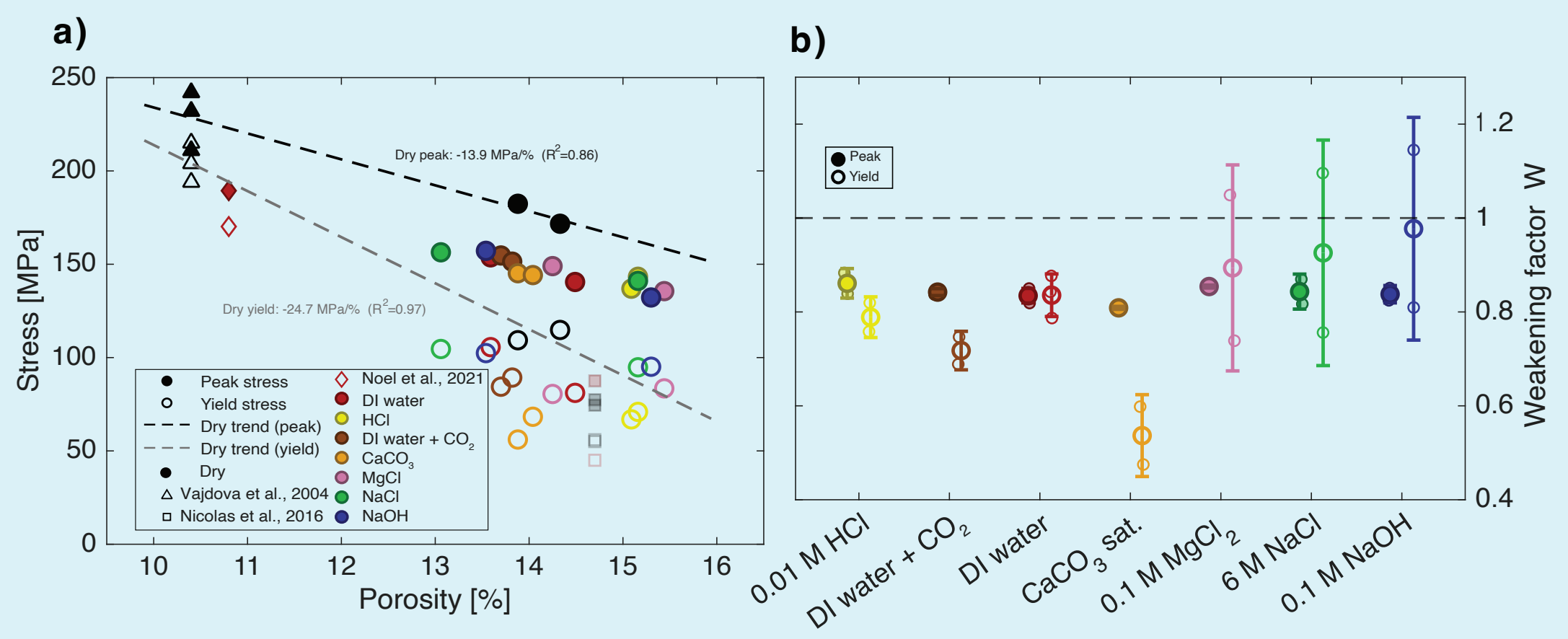

Figure 9: a) Peak and yield stress versus porosity of all the experiments on Tavel limestone performed at 20 MPa. b) Weakening compeared to the dry strength accounting for porosity variation.

Both peak and yield stress are strongly sensitive to porosity. To isolate the effect of fluid presence and chemistry, we normalize each saturated experiment by the dry stress predicted at its specific porosity.
Samples deformed with the **$CaCO_3$** solution show a 50% weakening in yield stress, compared to 20% of deionized water, but the same peak stress weakening of deionized water, around 20%. Samples deformed with **HCl** and **water + CO_2** show a similar behaviour with a yield weakening of 25 and 30%, respectively.
We propose that the lower yield stress in **$CaCO_3$**-saturated solution reflects: (1) the absence of crack-tip blunting, which lowers the stress required to propagate existing cracks, and (2) early onset of pressure solution, since the pore fluid is already at calcite saturation from the start of deformation.

Ductile deformation

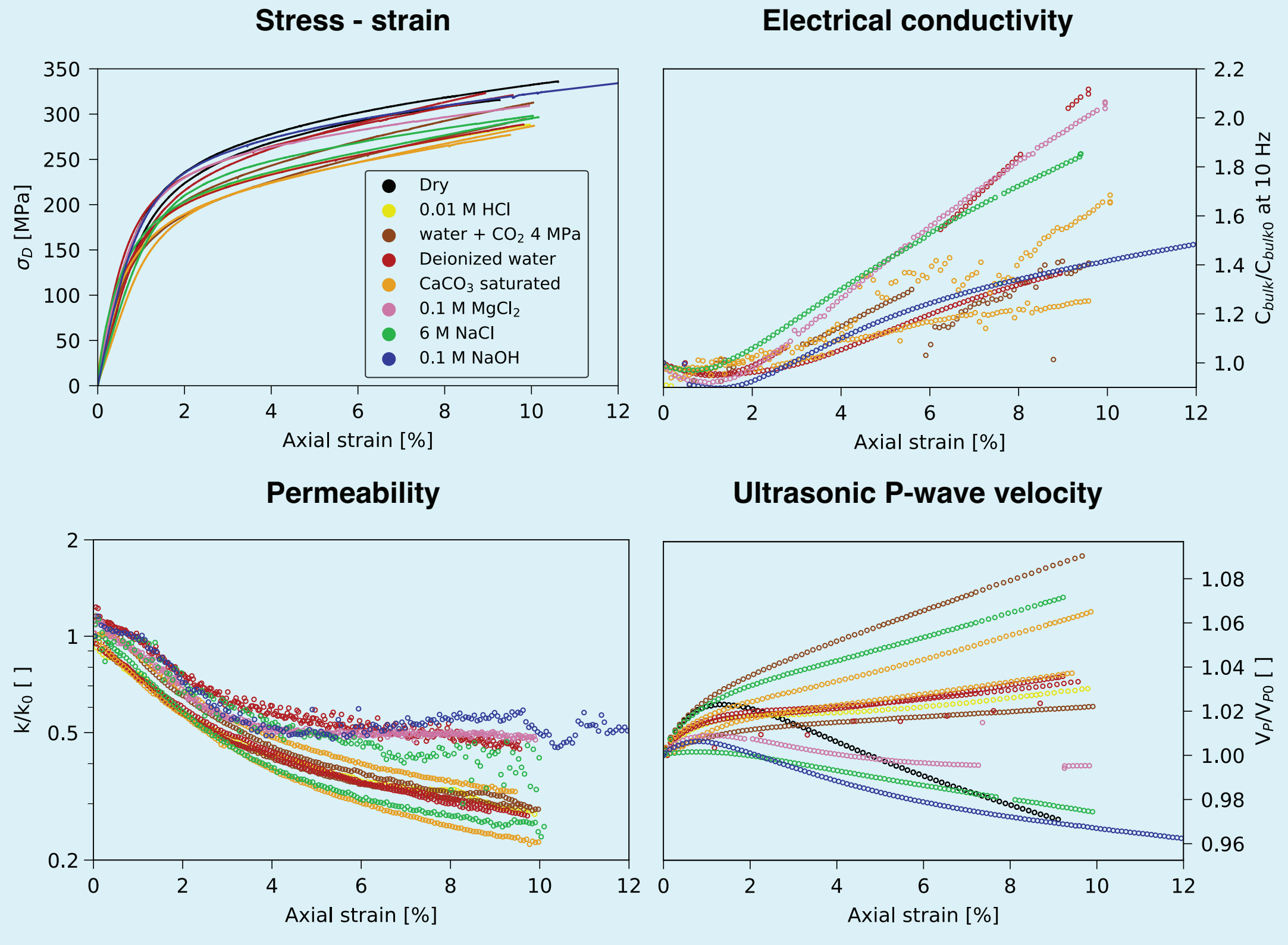

Figure 10: mechanical and physical measurements from experiments performed at $P_{c\ eff}$ = 100 MPa

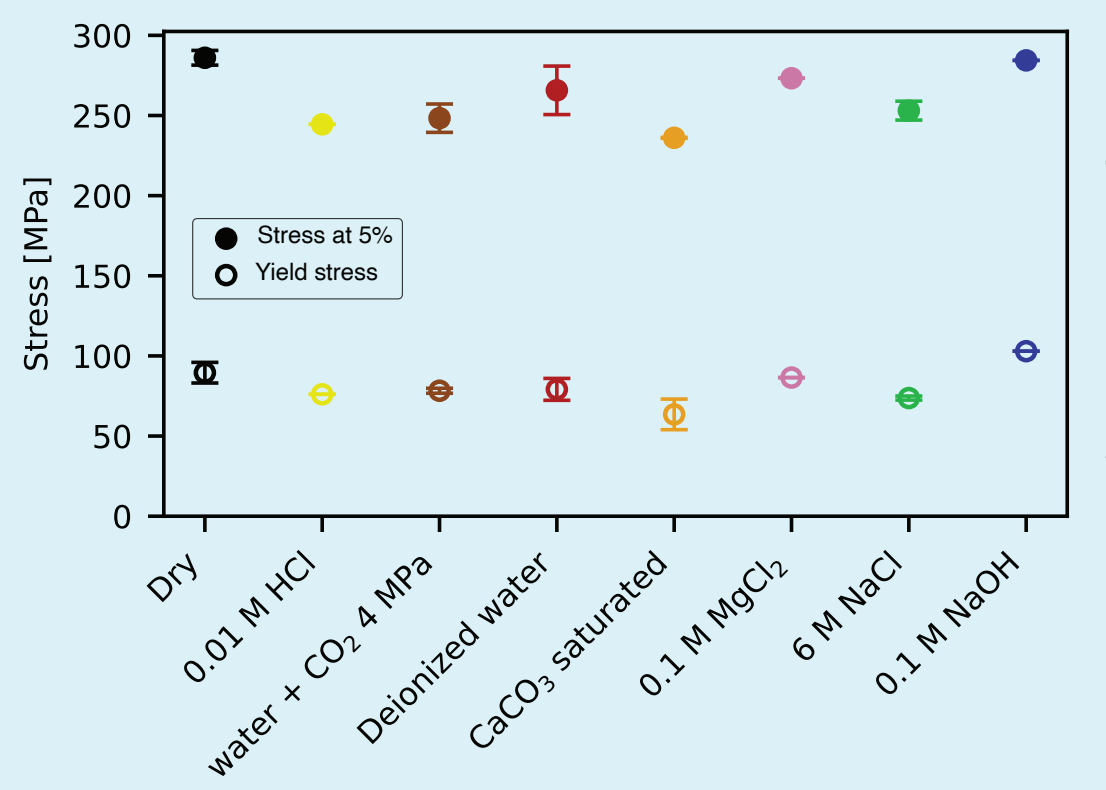

Samples saturated with a fluid show variable behaviour, with the stress of saturated samples falling between no weakening and 40% weakening. Permeability decreases during all the experiments, while electrical conductivity decreases until yielding, to increase with plastic deformation. V_P shows a variable behaviour as well, either increasing or decreasing with deformation, albeit with a small variation that could be justified by anisotropies in the samples.

Microstructures

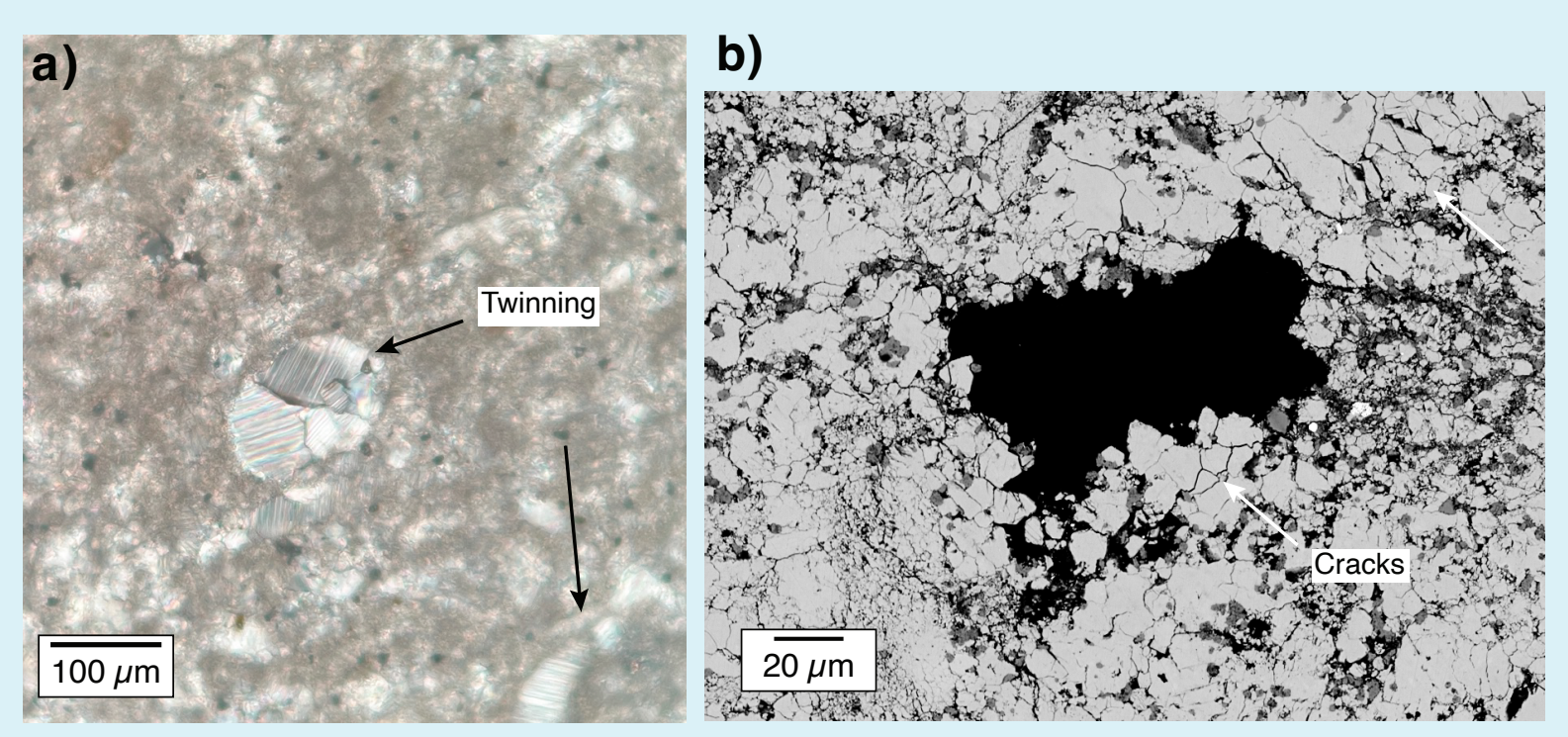

Samples deformed at 100 MPa show pervasive cracking and twinning, and less pores than the undeformed material.

Figure 11: a) oprical microscope image of twinned crystals in a sample deformed at 100 MPa with deionized water. b) SEM BSE image of cracks surrounding a pore in a sample deformed at 100 MPa wih DI water

Porosity effect

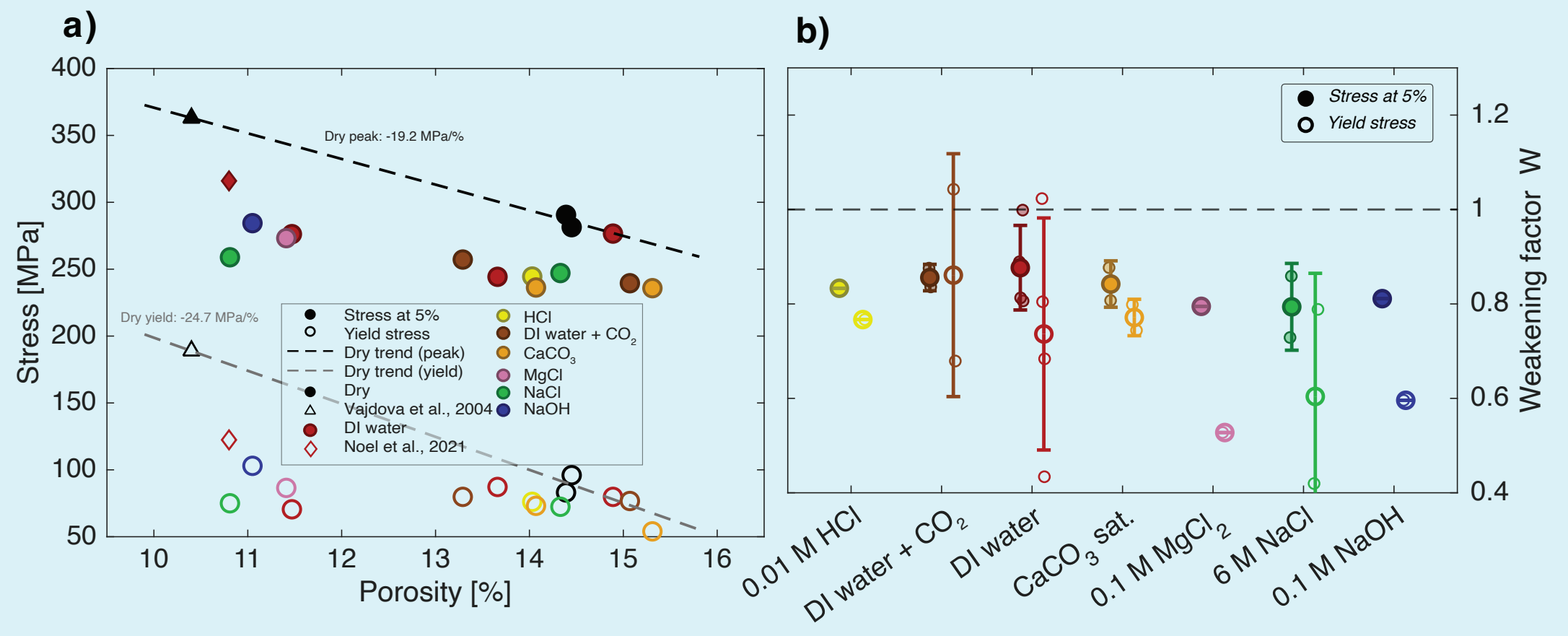

Figure 12: a) Stress at 5% strain and yield stress versus porosity of all the experiments on Tavel limestone performed at 100 MPa. b) Weakening compeared to the dry strength accounting for porosity variation.

Samples saturated with a fluid show large variability between replicates, preventing an identification of eventual differences between fluid chemistries. Weakening spans from 60% to 10% strengthening.

Micromechanical models

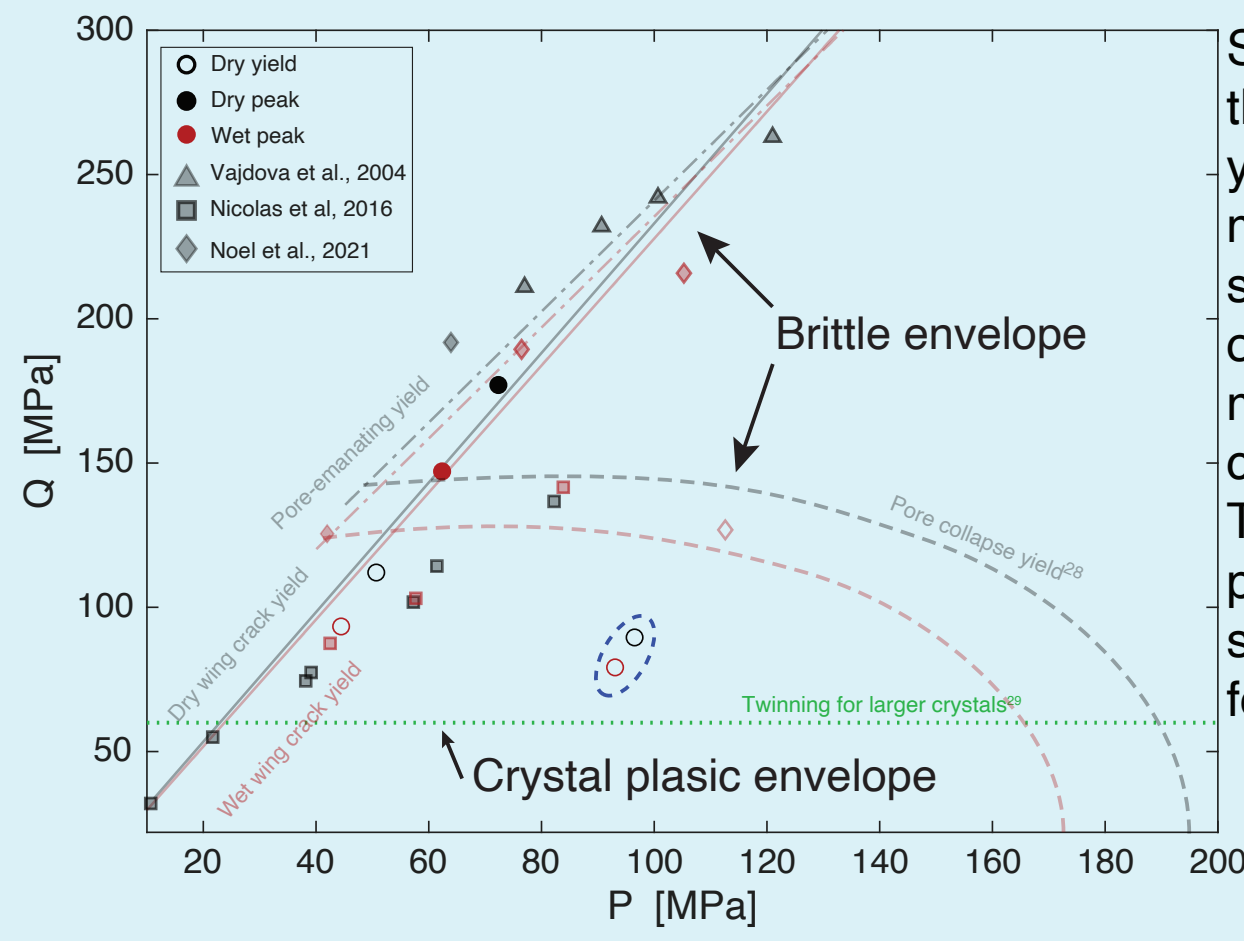

Samples deformed at lower P fall around the wing crack and pore emanating crack yield envelope. At higher P, all brittle models overestimate the measured strength. Given the high amount of twins observed in the microstructures, deformation is not accomodated by brittle processes only.
The insensitivity of twinning to pore fluid presence or chemistry can explain the smaller effect of fluids during ductile deformation.

Figure 13: Brittle and crystal plastic micromechanical models for yield stress prediction on Tavel limestone.

Conclusions

Localized deformation

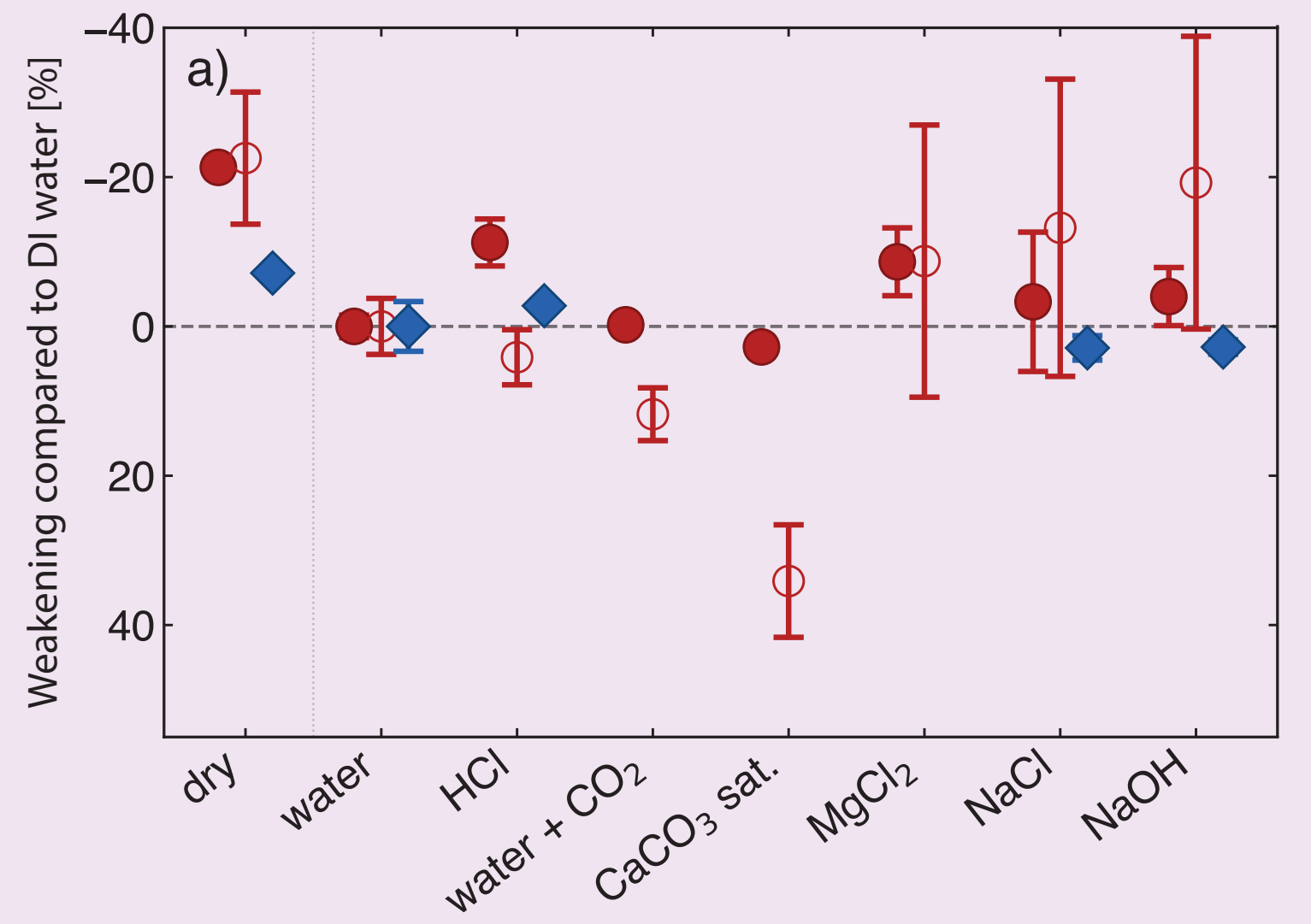

Figure 14: Peak and yield stress weakening for different pore fluid chemistry of Tavel limestone compared to a silicatic sandstone.

Tavel limestone deforming in the localized regime shows stronger water weakening than a silicatic sandstone under the same conditions[19]. Notably, samples saturated with **$CaCO_3$** solution show the largest yield weakening of the dataset (~50%, compared to ~20% for deionized water). We attribute this to the absence of crack-tip blunting: unlike the other fluids, the equilibrated solution does not dissolve crack tips, allowing cracks to propagate at lower stress. Once crack propagarion is initiated, however, the stress required to bring the sample to failure does not substantially change.

Ductile deformation

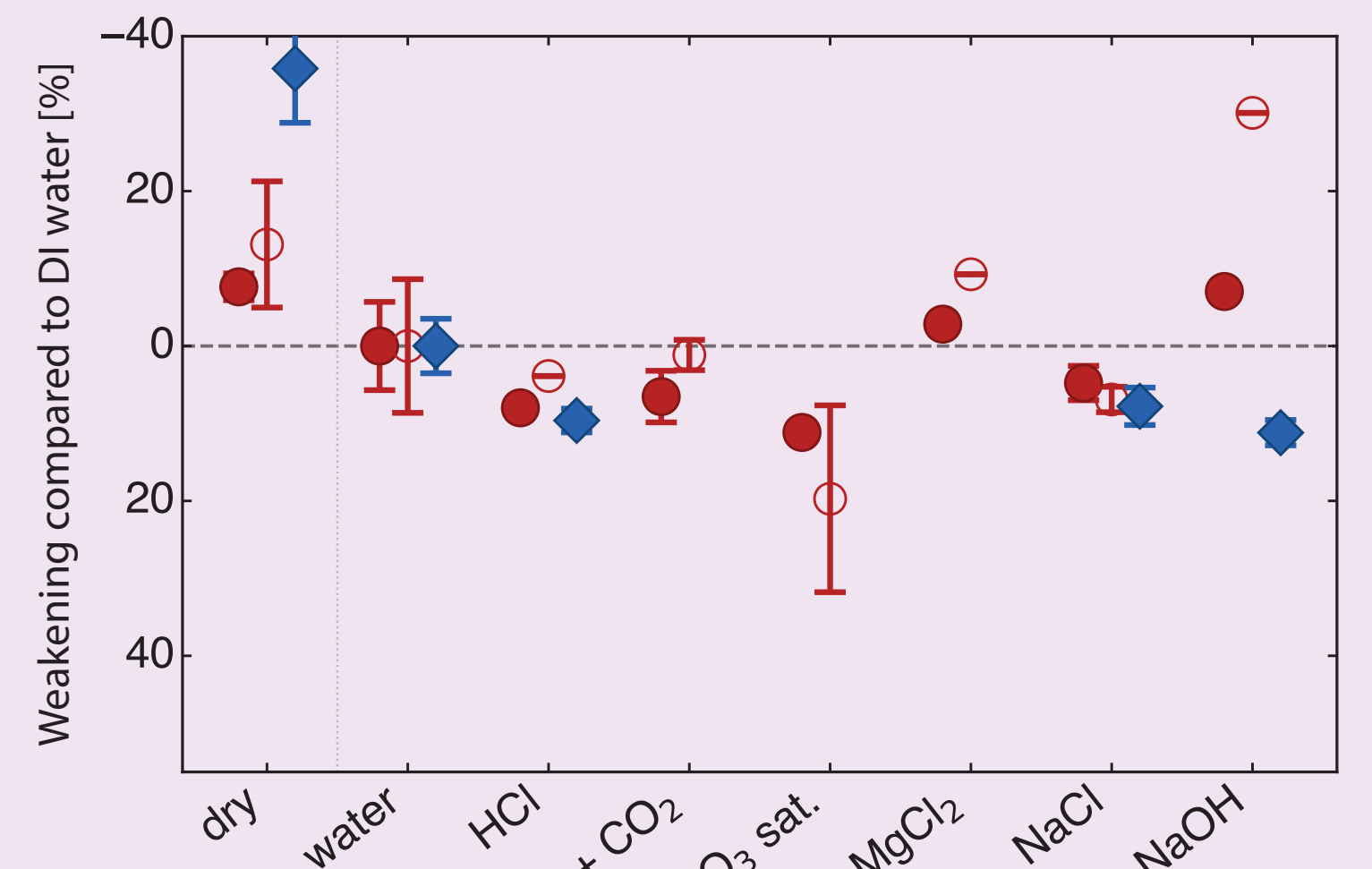

Figure 15: Stress at 5 or 3% strain and yield stress weakening for different pore fluid chemistry of Tavel limestone compared to a silicatic sandstone.

While a silicatic sandstone has been shown to be weakened by both flluid presence and chemistry when deforming in the ductile regime[19], Tavel limestone is less sensitive to fluid presence. Samples deformed with a **$CaCO_3$ saturated** solution induces the largest weakening out of the solutions tested, while a **NaOH** solution leads to a strength comparable to the dry samples.
We propose that the coexistance of several micromechanical processes and their different sensitivity to fluid chemistry leads to a complicated response of porous carbonate rocks to fluid chemistry.

- **Water weakening in carbonatic rocks is rock- and deformation regime-specific.**
- **Elecrical conductivity and V_P poentially indicate onset of dilatancy.**
- **Tavel limestone shows 20% water weakening regardless of the regime, the exposure to a $CaCO_3$-saturated solution can reduce yield stress down to 50% of its dry value, while the exposure to a basic soluion decreases weakening.**
- **The coexistance of several micromechanisms during deformation make predicting the effect of fluid chemistry on porous carbonates challenging.**

References

[1]Vajdova, V., Baud, P., & Wong, T. F. (2004). Permeability evolution during localized deformation in Bentheim sandstone. JGR: SE, 109(B10).
[2]Nicolas, A., Fortin, J., Regnet, J. B., Dimanov, A., & Guéguen, Y. (2016). Brittle and semi-brittle behaviours of a carbonate rock: influence of water and temperature. GJI, 206(1), 438-456.
[3]Noël, C., Passelègue, F. X., & Violay, M. (2021). Brittle faulting of ductile rock induced by pore fluid pressure build-up. JGR: SE, 126(3).
[4]Noël, C., Fryer, B., Baud, P., & Violay, M. (2024). Water weakening and the compressive brittle strength of carbonates: Influence of fracture toughness and static friction. International Journal of Rock Mechanics and Mining Sciences, 177, 105736.
[5] Lisabeth, H. P., & Zhu, W. (2015). Effect of temperature and pore fluid on the strength of porous limestone. JGR: SE, 120(9), 6191-6208.
[6] Baud, P., Hall, S., Heap, M. J., Ji, Y., & Wong, T. F. (2021). The brittle-ductile transition in porous limestone: Failure mode, constitutive modeling of inelastic deformation and strain localization. JGR: SE, 126(5).
[7]Baud, P., Schubnel, A., Heap, M., & Rolland, A. (2017). Inelastic compaction in high-porosity limestone monitored using acoustic emissions. JGR: SE, 122(12), 9989-10.
[8]Baud, P., Schubnel, A., & Wong, T. F. (2000). Dilatancy, compaction, and failure mode in Solnhofen limestone. JGR: SE, 105(B8), 19289-19303.
[9]French, M. E., Zhu, W., Xiao, X., Evans, B., & Prior, D. J. (2022). Thermally enhanced water weakening of the solnhofen limestone. JGR: SE, 127(3).
[10]Le Guen, Y., Renard, F., Hellmann, R., Brosse, E., Collombet, M., Tisserand, D., & Gratier, J. P. (2007). Enhanced deformation of limestone and sandstone in the presence of high fluids. JGR: SE 112(B5).
[11]Rimmelé, G., Barlet-Gouédard, V., & Renard, F. (2010). Evolution of the petrophysical and mineralogical properties of two reservoir rocks under thermodynamic conditions relevant for CO2 geological storage at 3 km depth. Oil & Gas Science and Technology–Revue de l'Institut Français du Pétrole, 65(4), 565-580.
[12]Grgic, D. (2011). Influence of CO2 on the long-term chemomechanical behavior of an oolitic limestone. JGR: SE, 116(B7).
[13]Castagna, A., Ougier-Simonin, A., Benson, P. M., Browning, J., Walker, R. J., Fazio, M., & Vinciguerra, S. (2018). Thermal damage and pore pressure effects of the Brittle-Ductile transition in comiso limestone. JGR: SE, 123(9), 7644-7660.
[14]Pluymakers, A., Ougier-Simonin, A., & Barnhoorn, A. (2021). Ion-species in pore fluids with opposite effects on limestone fracturing. Geomechanics for Energy and the Environment, 26, 100233.
[15]Bemer, E., Nguyen, M. T., Dautriat, J., Adelinet, M., Fleury, M., & Youssef, S. (2016). Impact of chemical alteration on the poromechanical properties of carbonate rocks. Geophysical Prospecting, 64(4-Advances in Rock Physics), 810-827.
[16]Sari, M., Sarout, J., Poulet, T., Dautriat, J., & Veveakis, M. (2022). The brittle–ductile transition and the formation of compaction bands in the Savonnières limestone: impact of the stress and pore fluid. Rock Mechanics and Rock Engineering.
[17]Xie, S. Y., Shao, J. F., & Xu, W. Y. (2011). Influences of chemical degradation on mechanical behaviour of a limestone. International Journal of Rock Mechanics and Mining Sciences, 48(5), 741-747.
[18]Kortram, J. D., Barnhoorn, A., & Pluymakers, A. (2023). Laboratory experiments on the effects of corrosion inhibitor on the mechanical properties of reservoir rock. Geothermal Energy, 11(1), 17.
[19]Lazari, F., Meyer, G., Baumgartner, L., & Violay, M. (2025). Fluid chemistry effect on localized and ductile deformation of a porous sandstone. Journal of Geophysical Research: Solid Earth, 130(8).
[20]Meyer, G. G., & Violay, M. (2023). Bounding the localized to ductile transition in porous rocks: implications for geo-reservoirs. Geophysical Journal International, 235(3), 2361-2371.
[21]Noël, C., Baud, P., & Violay, M. (2021). Effect of water on sandstone's fracture toughness and frictional parameters: Brittle strength constraints. International Journal of Rock Mechanics and Mining Sciences, 147.
[22]Rostom, F., Røyne, A., Dysthe, D. K., & Renard, F. (2013). Effect of fluid salinity on subcritical crack propagation in calcite. Tectonophysics, 583, 68-7
[23]Bergsaker, A. S., Røyne, A., Ougier-Simonin, A., Aubry, J., & Renard, F. (2016). The effect of fluid composition, salinity, and acidity on subcritical crack growth in calcite crystals. Journal of Geophysical Research: Solid Earth, 121(3), 1631-1651.
[24]Ilgen, A. G., Mook, W. M., Tigges, A. B., Choens, R. C., Artyushkova, K., & Jungjohann, K. L. (2018). Chemical controls on the propagation rate of fracture in calcite. Scientific reports, 8(1).
[25]Zhang, X., & Spiers, C. J. (2005). Compaction of granular calcite by pressure solution at room temperature and effects of pore fluid chemistry. International Journal of Rock Mechanics and Mining Sciences, 42(7-8), 950-960.
[26]Zhang, X., Spiers, C. J., & Peach, C. J. (2010). Compaction creep of wet granular calcite by pressure solution at 28 C to 150 C. Journal of Geophysical Research: Solid Earth, 115(B9).
[27]Diao, Y., Li, A., & Espinosa-Marzal, R. M. (2020). Ion specific effects on the pressure solution of calcite single crystals. Geochimica et Cosmochimica Acta, 280, 116-129.
[28]Zhu, W., Baud, P., & Wong, T. F. (2010). Micromechanics of cataclastic pore collapse in limestone. Journal of Geophysical Research: Solid Earth, 115(B4).
[29]Lacombe, O., Parlangeau, C., Beaudoin, N. E., & Amrouch, K. (2021). Calcite twin formation, measurement and use as stress–strain indicators: A review of progress over the last decade. Geosciences, 11(11), 445.